

# The Binding Sites for Competitive Antagonistic, Allosteric Antagonistic, and Agonistic Antibodies to the I Domain of Integrin LFA-1<sup>1</sup>

Chafen Lu,<sup>2</sup> Motomu Shimaoka, Azucena Salas, and Timothy A. Springer<sup>3</sup>

We explore the binding sites for mAbs to the  $\alpha$  I domain of the integrin  $\alpha_L\beta_2$  that can competitively inhibit, allosterically inhibit, or activate binding to the ligand ICAM-1. Ten mAbs, some of them clinically important, were mapped to species-specific residues. The results are interpreted with independent structures of the  $\alpha_L$  I domain determined in seven different crystal lattices and in solution, and which are present in three conformational states that differ in affinity for ligand. Six mAbs bind to adjacent regions of the  $\beta 1$ - $\alpha 1$  and  $\alpha 3$ - $\alpha 4$  loops, which show only small (mean, 0.8 Å; maximum, 1.8 Å) displacements among the eight I domain structures. Proximity to the ligand binding site and to noncontacting portions of the ICAM-1 molecule explains competitive inhibition by these mAbs. Three mAbs bind to a segment of seven residues in the  $\beta 5$ - $\alpha 6$  loop and  $\alpha 6$  helix, in similar proximity to the ligand binding site, but on the side opposite from the  $\beta 1$ - $\alpha 1/\alpha 3$ - $\alpha 4$  epitopes, and far from noncontacting portions of ICAM-1. These residues show large displacements among the eight structures in response to lattice contacts (mean, 3.6 Å; maximum, 9.4 Å), and movement of a buried Phe in the  $\beta 5$ - $\alpha 6$  loop is partially correlated with affinity change at the ligand binding site. Together with a lack of proximity to noncontacting portions of ICAM-1, these observations explain variation among this group of mAbs, which can either act as competitive or allosteric antagonists. One agonistic mAb binds distant from the ligand binding site of the I domain, to residues that show little movement (mean, 0.5 Å; maximum, 1.0 Å). Agonism by this mAb is thus likely to result from altering the orientation of the I domain with respect to other domains within an intact integrin  $\alpha_L\beta_2$  heterodimer. *The Journal of Immunology*, 2004, 173: 3972–3978.

Antibodies are widely used to study ligand binding by proteins. For example, in the fields of immunology and cell adhesion, mAbs are frequently selected and used in experimental studies based on their ability to inhibit or stimulate receptor-ligand interactions. However, the relationship between the Ab epitope and the receptor-ligand interface is often unknown. In this study, we examine this relationship in the particularly biologically interesting case of Abs to an integrin inserted (I)<sup>4</sup> domain, which exists in multiple conformational states that regulate affinity for ligands.

The integrin LFA-1 ( $\alpha_L\beta_2$ , CD11a/CD18) binds to ICAM-1, -2, and -3, and regulates adhesive functions and migration of lymphocytes and most other leukocytes (1, 2). Like many integrins, the adhesiveness of LFA-1 is dynamically regulated by signals from the cytoplasm (inside-out signaling) (3, 4). Many integrin  $\alpha$  subunits, including  $\alpha_L$ , contain an I domain of ~200 aa. The I domain mediates ligand binding by I domain-containing integrins (2). The I domain adopts the von Willebrand factor A domain/dinucleotide-

binding fold similar to that of small G proteins, and has a unique divalent cation coordination site designated the metal ion-dependent adhesion site (MIDAS).

Integrin I domains exist in so-called open and closed conformations, and a recently described intermediate conformation, that differ in affinity for ligand (4–6). Mutationally introduced disulfide bonds have been used to stabilize the  $\alpha_L$  I domain in a high affinity open conformation and an intermediate affinity intermediate conformation (6–8). The affinity for ICAM-1 of I domains mutationally stabilized in the open and intermediate conformations is 10,000-fold and 500-fold higher, respectively, than the closed conformation. The closed conformation is energetically favorable for the isolated wild-type I domain. The affinity and kinetics of the “locked open” isolated I domain for ICAM-1 are within experimental error of values obtained for active intact  $\alpha_L\beta_2$  (8, 9), showing that the binding site for ICAM-1 is contained wholly within the I domain. Multiple structures are available for the  $\alpha_L$  I domain in each of these conformational states, including one structure of a complex between the  $\alpha_L$  I domain and ICAM-1 (6, 10–13).

Numerous mAbs to the  $\alpha_L$  and  $\beta_2$  subunits of LFA-1 have been well characterized functionally. Many inhibit ligand binding, and a few are stimulatory (14–17). Furthermore, studies with  $\alpha_L\beta_2$  containing an I domain locked in the high affinity conformation have revealed distinct classes of inhibitory mAbs (18). All tested mAbs to the  $\beta_2$  I-like domain that inhibit binding to ICAM-1 of wild-type  $\alpha_L\beta_2$  fail to inhibit binding of  $\alpha_L\beta_2$  with the mutant high affinity, locked open I domain. This finding demonstrates that the  $\beta_2$  I-like domain has a regulatory, rather than direct, role in ligand binding, and further suggests that mAbs to the  $\beta_2$  I-like domain are allosteric rather than competitive antagonists. In the same study, mAbs to the  $\alpha$  I domain fell into two classes. One class inhibits both wild-type and locked open  $\alpha_L\beta_2$ , whereas the other inhibits only

CBR Institute for Biomedical Research, Department of Pathology, Harvard Medical School, Boston, MA 02115

Received for publication March 31, 2004. Accepted for publication June 25, 2004.

The costs of publication of this article were defrayed in part by the payment of page charges. This article must therefore be hereby marked *advertisement* in accordance with 18 U.S.C. Section 1734 solely to indicate this fact.

<sup>1</sup> This work was supported by National Institutes of Health Grant CA31798.

<sup>2</sup> Current address: Millennium Pharmaceuticals, 75 Sidney Street, Cambridge, MA 02139.

<sup>3</sup> Address correspondence and reprint requests to Dr. Timothy A. Springer, CBR Institute for Biomedical Research, Department of Pathology, Harvard Medical School, 200 Longwood Avenue, Boston, MA 02115. E-mail address: springeroffice@cbr.med.harvard.edu

<sup>4</sup> Abbreviations used in this paper: I domain, inserted domain; MIDAS, metal ion-dependent adhesion site.

wild-type  $\alpha_L\beta_2$ . These findings suggest that mAbs to the  $\alpha$  I domain may function either as competitive or allosteric antagonists (18). A third class of mAb to the  $\alpha_L$  I domain enhances binding to ICAM-1 (17, 19).

Despite these observations, the basis of agonism and the two different classes of antagonism remain unclear. Stimulated by the availability of structures of the  $\alpha_L$  I domain in different conformational states and in complex with ICAM-1 (6), we have mapped I domain epitopes to individual species-specific amino acid residues to gain insights into how mAb to the I domain can either competitively inhibit, allosterically inhibit, or stimulate binding to ICAM-1. The mechanism of action of mAb to the  $\alpha_L$  I domain is also of great interest clinically, because such mAb can prevent graft-vs-host disease following bone marrow transplantation (20), and clinically benefit patients with moderate to severe plaque psoriasis (21).

## Materials and Methods

### Monoclonal Abs

The mouse anti-human  $\alpha_L$  (CD11a) mAbs TS1/11, TS1/12, TS1/22, TS2/4, TS2/6, TS2/14, mouse anti- $\beta_2$  (CD18) mAb TS1/18, and the nonbinding myeloma IgG X63 were described previously (22). mAbs F8.8, BL5, May.035 (23), 25-3-1 (24), and CBR LFA-1/9 (25) were obtained through the 5th International Leukocyte Workshop (26). mAb MEM83 (17, 19) was generously provided by Dr. V. Horejsi (Institute of Molecular Genetics, Prague, Czech Republic).

### Cell lines

Human embryonic kidney 293T cells were cultured in DMEM medium supplemented with 10% FBS, 2 mM glutamine, and 50  $\mu$ g/ml gentamicin. Stable K562 cell lines that express wild-type LFA-1 or the isolated  $\alpha_L$  I domain were described previously (7).

### cDNA construction and expression

Human and mouse  $\alpha_L$  chimeras in expression vector AprM8 were described previously (14).

Overlap extension PCR (27, 28) was used to generate single or multiple human-to-mouse substitution mutations in the  $\alpha_L$  I-domain. Wild-type  $\alpha_L$  cDNA in AprM8 was used as template for the first PCR. The outer left

primer for PCR extension was complementary to vector sequence containing the *EcoRI* site in the multiple cloning site 5' to the  $\alpha_L$  cDNA, and the outer right primer was 3' to the *EcoRI* site at nt 1818 near the middle of the coding region of the  $\alpha_L$  cDNA. The inner primers were designed for each individual mutation and contained overlapping sequences. The final PCR products with outer primers were digested with *EcoRI* and used to replace the corresponding fragment in the wild-type  $\alpha_L$  cDNA in AprM8. Clones with the correct orientation were selected, and the entire inserted segment was sequenced to confirm its correctness.

Wild-type or mutant  $\alpha_L$  cDNA was transiently cotransfected with wild-type  $\beta_2$  cDNA in vector AprM8 in 293T cells as described (29). Two days after transfection, cells were harvested for flow cytometric analysis.

### Flow cytometry

Flow cytometry was as described (29). mAb TS1/11, TS1/12, and the non-binding IgG X63 were used as hybridoma supernatants at 1/20 dilution, mAbs TS1/22, TS2/4, TS1/18, and MEM83 at 15  $\mu$ g/ml purified IgG, and the International Leukocyte Workshops mAbs F8.8, BL5, May.035, 25-3-1, and CBR LFA-1/9 were used at 1/100 dilution.

## Results

Epitope expression was examined by cotransfection of mutant or wild-type  $\alpha_L$  cDNA and wild-type  $\beta_2$  cDNA in 293T cells followed 2 days later by staining with mAb, FITC anti-mouse IgG, and quantitative immunofluorescence flow cytometry. For each mutation, at least two independent clones were tested by transfection, and expression was measured in at least three independent transfections. Representative  $\alpha_L\beta_2$  293T transfectant flow cytometry histograms have previously been shown (29). The nine function-blocking mAbs studied here have previously been mapped using  $\alpha_L$  chimeras in which six different I domain segments of 30 to 60 residues were replaced with mouse sequence (14). These previous results with the chimeras were confirmed (Tables I and II), and the activating mAb MEM83 was also mapped to the same segments (Table III). Segments of mouse sequence that resulted in reduced reactivity were subdivided into subregions, and subregions showing reduced reactivity were further dissected into individual human-to-mouse amino acid substitutions. All mutants studied here were expressed equally as well as wild-type  $\alpha_L\beta_2$ , and were expressed as  $\alpha_L\beta_2$  complexes, as shown by mAb TS2/4 that

Table I. Competitive antagonistic Abs to the  $\beta_1$ - $\alpha_1$  and  $\alpha_3$ - $\alpha_4$  loops<sup>a</sup>

Human-to-Mouse Substitution	F8.8	CBR LFA-1/9	BL5	May.035	TS1/11	TS1/12	Reactivity												
h118m153h	—	—	—	+++++	+++++	+++++													
P144R	—	—	—	ND	ND	ND													
h153m183h	+++++	+++++	+++++	+++++	+++++	+++++													
h184m215h	—	—	—	—	—	—													
R189N/D191N	+++++	+++++	+++++	+++++	+++++	+++++													
A194V/K197G/H198S	+++++	+++++	—	+	—	—													
A194V	+++++	+++++	+++++	+++++	+++++	+++++													
K197G	+++++	+++++	+	+	—	—													
H198S	+++++	+++++	+++++	+++++	+++++	+++++													
K200Q/H201P/L203F	—	—	+	—	—	—													
K200Q	—	—	+++++	+++++	+++++	+++++													
H201P	—	++	+	++	—	—													
L203F	+++++	+++++	+++++	+++++	++	++													
G210R	+++++	+++++	+++++	+++++	+++++	+++++													
h217m248h	+++++	+++++	+++++	+++++	+++++	+++++													
h249m303h	+++++	+++++	+++++	+++++	+++++	+++++													
h300m359h	+++++	+++++	+++++	+++++	+++++	+++++													
Epitope	P144	P144	P144	K197	K197	K197													
	K200	K200	K197	H201	H201	H201													
	H201	H201	H201		L203	L203													

<sup>a</sup> Mean-specific fluorescence intensity, i.e., with background X63 IgG1 fluorescence intensity subtracted, for each mutant Ab was determined as percentage of wild type, and averaged for all independent transfections ( $n \geq 3$ ). +++++, comparable to wild type; ++++, 70–90% of wild type; ++, 50–70% of wild type; +, 30–50% of wild type; —, < 30% of wild type; —, indistinguishable from the X63 control.

Table II. Competitive and allosteric antagonistic Abs to the  $\beta 5$ - $\alpha 6$  loop and  $\alpha 6$  helix<sup>a</sup>

Human-to-Mouse Substitution	TS1/22	TS2/14	25-3-1
	Reactivity		
h118m153h	+++++	+++++	+++++
h153m183h	+++++	+++++	+++++
h184m215h	+++++	+++++	+++++
h217m248h	+++++	+++++	+++++
h249m303h	—	—	—
D249S/K252H	+++++	+++++	+++++
I255H	+++++	+++++	+++++
Q266V/T267S/K268V/ E269Q/S270K/E272K	—	+	—
Q266V	—	+++++	—
T267S	+++++	+++++	+++
K268V	+++++	+++++	+++
E269Q	+++++	+++++	+++++
S270K	++	++	+
E272K	+++++	+++	++
K276I	+++++	+++++	+++++
K280E/A282V/S283E	+++++	+++++	+++++
h300m359h	+++++	+++++	+++++
Epitope	Q266 S270	S270 E272	Q266 T267 K268 S270 E272
Class	competitive	allosteric	allosteric

<sup>a</sup> See legend to Table I.

maps to the  $\alpha_L$   $\beta$ -propeller domain and requires  $\beta_2$  association for reactivity (30).

Six of the inhibitory mAbs require human residues 185–215 for reactivity, and three of these also require residues 119–153 (Table I). Single amino acid substitutions had already been prepared in the 119–153 subregion, and as previously described (14), only the Pro<sup>144</sup>→Arg substitution in this subregion affected binding, and it completely abolished binding of all three mAb (Table I). Within the region of residues 184–215, four of the mAbs require human residues in subregion 194–198 (Table I). Individual substitutions show that residue Lys<sup>197</sup> is the only species-specific residue required in this subregion. All six of the mAbs require the subregion of residues 200–203 (Table I), which includes species specific residues Lys<sup>200</sup>, His<sup>201</sup>, and Leu<sup>203</sup>. Individual substitutions show that two Abs require Lys<sup>200</sup>, all six require His<sup>201</sup>, and a different subset of two Abs requires Leu<sup>203</sup>. Thus, the six mAb map to four distinct epitopes (Table I, bottom row), all contained within the structurally contiguous  $\beta 1$ - $\alpha 1$  and  $\alpha 3$ - $\alpha 4$  loops of the  $\alpha_L$  I domain (Fig. 1). These same loops each contain residues that contact ICAM-1 (Fig. 1), correlating with the observation that all six mAbs are competitive antagonists of ICAM-1 (18).

A different set of three antagonistic mAbs to the  $\alpha_L$  I domain require the segment containing residues 250–303 (Table II). Only the subregion of 266–272 affected Ab binding. Single amino acid substitutions show that mAb TS1/22 recognizes residues 266 and 270, mAb TS2/14 recognizes residues 270 and 272, and mAb 25-3-1 recognizes residues 266, 267, 268, 270, and 272. Thus, these three mAbs recognize three distinct epitopes in the  $\beta 5$ - $\alpha 6$  loop and the short  $\alpha 6$  helix (Fig. 1). This loop and helix are not far from the ICAM-1 binding site, undergo reshaping between the closed and open conformations, and also undergo reshaping as a consequence of crystal lattice contacts. These observations are not inconsistent with the ability of TS1/22 but not TS2/14 and 25-3-1 to strongly inhibit ligand binding by locked open  $\alpha_L\beta_2$  (see Discussion).

Table III. An agonistic Ab to the  $\beta 3$ - $\alpha 2$  loop and the  $\alpha 4$  helix<sup>a</sup>

Human-to-mouse substitution	MEM83 Reactivity
h118m153h	+++++
h153m183h	—
K159R	+++++
S176D/Y177C/K178R	+++++
S176D	+++++
Y177C	+++++
K178R	+++++
D182T/S184L	—
D182T	—
S184L	+++++
h184m215h	+++++
h217m248h	+
A216V/T217A/E218H	+++++
E218H	++++
R221K	+++++
L224S	+++++
I235V	+++++
T243S	+++++
S245K	+++++
h249m303h	+++++
h300m359h	+++++
Epitope	D182 E218

<sup>a</sup> See legend to Table I.

The agonistic mAb MEM83 requires two human regions, residues 153–183 and 217–248 (Table III). Only residue Asp<sup>182</sup> is required in the first region. In region 217–248, substitution Glu<sup>218</sup>→His lowered mAb MEM83 reactivity (Table III). Substitution of all residues in this region lowered reactivity more than Glu<sup>218</sup>→His, showing a combinatorial effect of one or more additional residues. The MEM83 epitope thus requires residues in the contiguous  $\beta 3$ - $\alpha 2$  loop and the  $\alpha 4$  helix, which locate far from the MIDAS (see below).

## Discussion

The use of mAbs to inhibit or stimulate cell-cell interactions is widespread, particularly in immunology, and far-reaching conclusions are drawn from such studies. We have attempted to understand the mechanism of action of a set of Abs to LFA-1 with different inhibitory or stimulatory effects that are widely used in the research literature and are of clinical importance. The epitopes for 10 such mouse anti-human integrin  $\alpha_L$  Abs have been mapped in this study using human-to-mouse species-specific amino acid substitutions. This information can now be evaluated with respect to the structure of a mutant intermediate affinity  $\alpha_L$  I domain complexed with domains 1 and 2 of ICAM-1 (6) (Fig. 2). A recent structure of a mutant high affinity  $\alpha_L$  I domain bound to domain 1 of ICAM-3 reveals an almost identical set of contact residues on the I domain, and an essentially identical orientation between the  $\alpha_L$  I domain and the ICAM.<sup>5</sup> Moreover, the information can also be evaluated with respect to eight independent  $\alpha_L$  I domain structures (Table IV). These structures are present in the three different conformational states termed closed, intermediate, and open, which regulate affinity of  $\alpha_L$  for ICAMs. They are also present in seven different crystal packings or in solution (Table IV), allowing conformational variation of loop structures, as influenced by crystal packing interactions, to be evaluated. What the epitope mapping together with the structural studies can teach us about the

<sup>5</sup> G. Song, Y. Yang, J.-H. Liu, T. Springer, and J.-H. Wang. Submitted for publication.

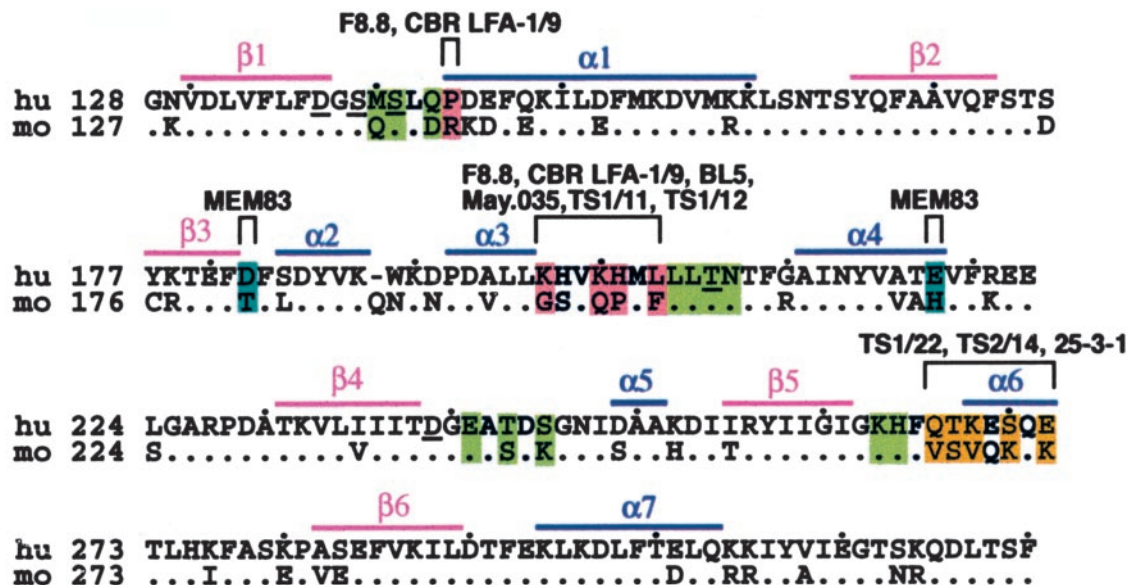


**FIGURE 1.** Alignment of the human and mouse  $\alpha_L$  I domains. Only residues that differ in the mouse are shown.  $\beta$  strands and  $\alpha$  helices are marked above the sequences. Epitopes are bracketed, and species-specific residues recognized by one or more mAbs are highlighted a different color for each of the three epitope groups. I domain residues contacting ICAM-1 in the crystal structure (6) are highlighted in green. Metal-coordinating MIDAS residues are underlined. Every 10th residue is dotted.

mechanism of inhibition or stimulation by the Abs is discussed for each of the three epitope groups in turn.

The epitopes in the  $\beta$ 1- $\alpha$ 1 and  $\alpha$ 3- $\alpha$ 4 loops recognized by mAbs F8.8, CBR LFA-1/9, BL5, May.035, TS1/11, and TS1/12, are located on the “top” and “side” faces of the  $\alpha_L$  I domain, close to the ICAM-1 binding site centered on the MIDAS (Fig. 2). Indeed, the  $\beta$ 1- $\alpha$ 1 and  $\alpha$ 3- $\alpha$ 4 loops each contain residues that coordinate the MIDAS metal ion and that contact ICAM-1 (Fig. 1). Although species-specific residues are present in ICAM-1 contacts in the  $\beta$ 1- $\alpha$ 1 and  $\beta$ 4- $\alpha$ 5 loops (Fig. 1), they are not recognized by any mAbs characterized to date. The mAbs to the  $\beta$ 1- $\alpha$ 1 and  $\alpha$ 3- $\alpha$ 4 loops all block ligand binding to  $\alpha_L\beta_2$  locked in the open, high affinity conformation as well as activated wild-type  $\alpha_L\beta_2$ , and thus appear to inhibit by a competitive rather than an allosteric mechanism (18). All of these mAbs recognize two or three species-specific residues in the  $\alpha$ 3- $\alpha$ 4 loop, and three of them additionally recognize Pro<sup>144</sup> in the  $\beta$ 1- $\alpha$ 1 loop (Fig. 1). In a previous study (31), three different mAbs were found to recognize Pro<sup>144</sup> and the  $\alpha$ 3- $\alpha$ 4 loop, similarly to F8.8, CBR LFA-1/9, and BL5 in this study. Furthermore, similarly to May.035, TS1/11, and TS1/12 in this study, MHM24 (32) was previously found to recognize residues Lys<sup>197</sup>, Lys<sup>200</sup>, and His<sup>201</sup> (Leu<sup>203</sup> was not tested) (31). The Ag-combining site of the MHM24 mAb has been grafted onto human V<sub>H</sub> and V<sub>L</sub> variable domain frameworks and constant domains to create the “humanized” Raptiva (efalizumab) Ab. Efalizumab has successfully completed several phase III clinical trials for moderate to severe psoriasis, and recently was approved by the Food and Drug Administration (21, 33). Like the other mAbs mapping to this region, MHM24 mAb blocks ligand binding by both locked open, high affinity  $\alpha_L\beta_2$ , and wild-type  $\alpha_L\beta_2$  (data not shown).

Three factors appear to be important to explain the finding that all tested mAbs to the  $\beta$ 1- $\alpha$ 1/ $\alpha$ 3- $\alpha$ 4 epitopes are competitive antagonists of ICAM-1 binding. First, there is little difference among the eight independent  $\alpha_L$  structures in this region. The deviations in C $\alpha$  atom positions of epitope residues average 0.6–0.9 Å, and do not exceed 1.8 Å among the eight structures (Table V). Furthermore, there is little movement in this region between the open

and closed conformations. The lack of structural variation in the  $\beta$ 1- $\alpha$ 1 and  $\alpha$ 3- $\alpha$ 4 loops from one structure to another, despite differing lattice contacts, suggests that these loops are relatively rigid. Therefore, there is little scope for Ab binding to perturb loop structure, and change the distance of the loops from the ICAM-1 binding site or change the orientation of the Ab binding site relative to the orientation of bound ICAM-1. Second, the ICAM-1 binding site is located very close to the  $\beta$ 1- $\alpha$ 1/ $\alpha$ 3- $\alpha$ 4 epitopes, as measured by either the distance between the nearest of the ICAM-1 contact and epitope residues, or the average distance of the nearest contact residue to all epitope residues (Table V). An average Ab-protein Ag recognition surface is  $\sim 800$  Å<sup>2</sup> (34), corresponding to a circle with a radius of  $\sim 15$  Å. Therefore, the ICAM-1 contact surface and the Ab contact surfaces in the  $\beta$ 1- $\alpha$ 1/ $\alpha$ 3- $\alpha$ 4 loops are predicted to overlap, or to be sufficiently close, so that a bound Ab Fab would occupy some of the same space as a bound ICAM-1. Third, ICAM-1 binds to the  $\alpha_L$  I domain with an orientation such that portions of domains 1 and 2 of ICAM-1 are very close to the  $\beta$ 1- $\alpha$ 1/ $\alpha$ 3- $\alpha$ 4 epitope and a bound Fab would project toward the junction between domains 1 and 2 (Fig. 2). Because the Fab portion of an Ab is  $\sim 100$  Å in diameter, an Ab to the  $\beta$ 1- $\alpha$ 1/ $\alpha$ 3- $\alpha$ 4 epitope would sterically block ICAM-1 binding even whether it did not necessarily occlude the contact site. This was confirmed by docking of a Fab to the epitope using molecular graphics.

We mapped mAbs TS1/22 and 25-3-1 to residues 266–272. It is puzzling that another study mapped the TS1/22 and 25-3-1 mAbs to a completely different site at residues Ile<sup>126</sup> and Asn<sup>129</sup>, in the linker between the  $\beta$ -propeller domain and I domain (31). In our own studies, the lack of reactivity of these mAbs with region 126–129 was previously (14), and in the present study, validated with  $\alpha_L$  chimeras m153h395m and/or h118m153h, which contained mouse residues in this region and were fully reactive with TS1/22 and 25-3-1 mAbs. Furthermore, mapping to residues 266–272 has been validated previously (14), and in the current study with  $\alpha_L$  chimeras h153m359, h249m303h, and Q266V/T267S/K268V/E269Q/S270K/E272K, and with absence or diminished reactivity with five different single amino acid substitution mutants in this region. In the other study (31), mapping to residues Ile<sup>126</sup> and



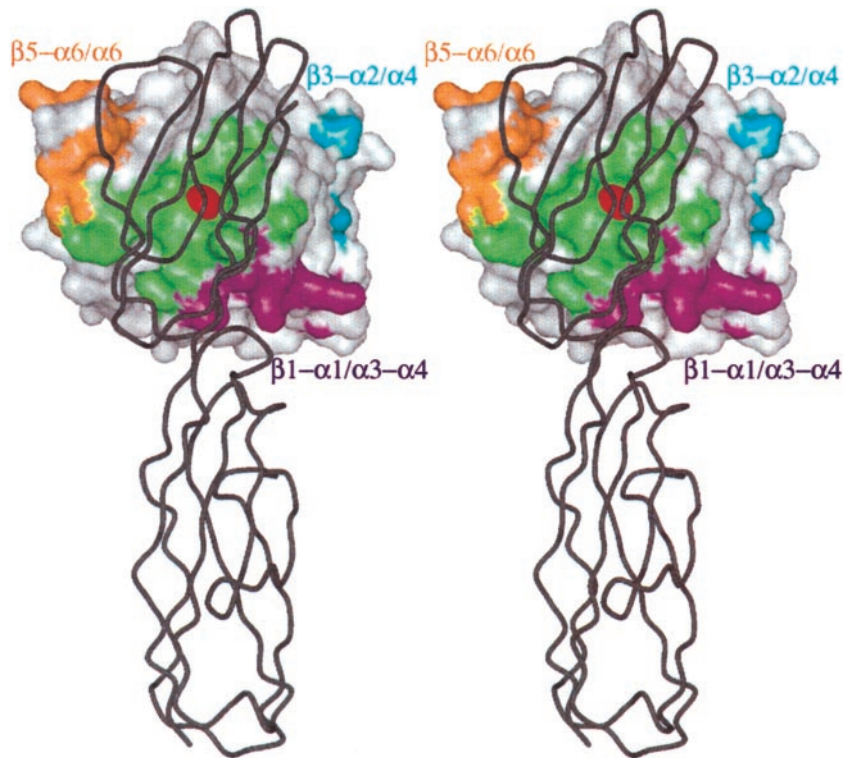


**FIGURE 2.** Stereodigram of the ICAM-1 contact surface and epitopes on the  $\alpha_L$  I domain. The  $\alpha_L$  I domain is shown as a molecular surface and ICAM-1 is shown as a black C $\alpha$  worm trace. Residues on the  $\alpha_L$  I domain with atoms within 3.5 Å of ICAM-1 are green and the MIDAS Mg $^{2+}$  is red. Species-specific residues in the epitopes are color coded the same as in Fig. 1: magenta for F8.8, CBR LFA-1/9, BL5, May.035, TS1/11, and TS1/12; orange for TS1/22, TS2/14, and 25-3-1; and cyan for MEM83. Figure prepared from the  $\alpha_L$  I domain complex with domains 1 and 2 of ICAM-1 (6) using GRASP (44), Bobsript (45), and Raster 3D (46).

Asn $^{129}$  was supported by only one  $\alpha_L$  chimera, termed H/M53, containing mouse residues in this region, and was counterindicated by the lack of effect by individual amino acid substitutions at Ile $^{126}$  and Asn $^{129}$ . Furthermore, no  $\alpha_L$  chimeras containing mouse substitutions covering the region 266–272 to which we map TS1/22 and 25-3-1 were studied (31). The effect of H/M53 was specific for particular Abs, and was particularly intriguing because it introduced mouse residues recognized by rat anti-mouse mAbs, M17/4 (35) and I21/7 (36); M17/4 is widely used to block  $\alpha_L\beta_2$  function in mouse models of disease (37, 38). Our mapping data suggest that chimera H/M53 inadvertently included mouse sequence in the region 266–272.

The mAbs TS1/22, TS2/14, and 25-3-1 recognize species-specific residues in the  $\beta 5$ - $\alpha 6$  loop and  $\alpha 6$  helix (hereinafter called the  $\beta 5$ - $\alpha 6/\alpha 6$  epitopes), on the opposite side of the MIDAS from the  $\beta 1$ - $\alpha 1/\alpha 3$ - $\alpha 4$  epitopes (Fig. 2). Despite mapping to similar epitopes, the TS1/22, TS2/14, and 25-3-1 mAbs differ considerably functionally. TS1/22 strongly inhibits ligand binding by all forms of  $\alpha_L\beta_2$  in all types of assays. In contrast, TS2/14 and 25-3-1 completely block adhesion to ICAM-1 of cells expressing activated wild-type  $\alpha_L\beta_2$ , but under identical conditions fail to block, or block only weakly, adhesion of cells expressing the locked open, high affinity  $\alpha_L$  K287C/K294C mutant in  $\alpha_L\beta_2$  heterodimers or the isolated I domain (18,

39). These findings suggest differences in the mode of inhibition, such as direct competition by TS1/22 mAb and allosteric or mixed competitive/noncompetitive inhibition by TS2/14 and 25-3-1 mAb. mAb 25-3-1 is important clinically; it has been used in multiple clinical studies to prevent graft-vs-host disease following bone marrow transplantation (20, 24).

Multiple factors appear to be important to explain the differences among mAbs to the  $\beta 5$ - $\alpha 6/\alpha 6$  epitopes and the finding that some of them act other than as competitive antagonists. First, there are large differences in the position of the epitopes among the eight independent  $\alpha_L$  structures, on average 3.0–3.9 Å/residue, and as much as 9.4 Å/residue (Table V). These differences are mostly attributable to crystal lattice contacts. There is no general correlation between the overall closed, intermediate, and open conformation of the  $\alpha_L$  I domain and  $\beta 5$ - $\alpha 6$  loop/ $\alpha 6$  helix conformation (6); however, Phe $^{265}$  within the  $\beta 5$ - $\alpha 6$  loop swings away from the  $\beta 4$ - $\alpha 5$  loop to accommodate the closed-to-open transition at the MIDAS (6). Phe $^{265}$  is in the  $\beta 5$ - $\alpha 6$  loop, immediately adjacent to both ICAM-1-contacting residues Lys $^{263}$  and His $^{264}$ , and  $\beta 5$ - $\alpha 6/\alpha 6$  epitope residues 266–272 (Fig. 1). The movement of Phe $^{265}$  provides a mechanism whereby an Ab-enforced conformation of the  $\beta 5$ - $\alpha 6$  loop could be allosterically coupled to the closed conformation of the  $\alpha_L$  I domain, resulting in an allosteric mechanism

Table IV.  $\alpha_L$  I domain structures

Protein Data Bank Code	Characteristics	Residue (Å)	Space Group	Unit Cell (a, b, c) (Å)	Reference
1LFA	Wild type	1.8	C2	131.1, 45.4, 66.1	10
1ZON	Wild type	2.0	P2 $_1$ 2 $_1$ 2 $_1$	63.1, 63.7, 40.2	11
1CQP	Wild type + antagonist	2.6	P2 $_1$ 2 $_1$ 2 $_1$	72.7, 77.7, 91.8	12
1DQG	Wild type in solution				13
1MJN	Intermediate affinity mutant	1.3	P2 $_1$ 2 $_1$ 2 $_1$	40.4, 57.4, 66.9	6
1MQ8	Intermediate affinity mutant + ICAM-1	3.3	P1	46.6, 62.9, 81.5	6
1MQA	High affinity mutant	2.5	C222 $_1$	61.9, 121.3, 54.1	6
1MQ9	High affinity mutant, pseudoliganded	2.0	P4 $_1$ 2 $_1$ 2 $_1$	35.6, 35.6, 269.6	6

Table V. Structural properties of  $\alpha_L$  I domain epitopes<sup>a</sup>

Region	Monoclonal Ab	Epitope	Mean Deviation between Structures (Å/residue)	Maximum Deviation between Structures (Å/residue)	Nearest ICAM-1 Contact Residue	Distance to Nearest Epitope Residue (Å)	Average Distance to Epitope Residue (Å)
$\beta 1$ - $\alpha 1/\alpha 3$ - $\alpha 4$	F8.8, CBR LFA-1/9	P144, K200, H201	0.7	1.2	Q143	3.7	10.4
$\beta 1$ - $\alpha 1/\alpha 3$ - $\alpha 4$	BL5	P144, K197, H201	0.9	1.8	Q143	3.7	12.6
$\beta 1$ - $\alpha 1/\alpha 3$ - $\alpha 4$	May.035	K197, H201	0.8	1.8	M140	9.2	16.2
$\beta 1$ - $\alpha 1/\alpha 3$ - $\alpha 4$	TS1/11, TS1/12	K197, H201, L203	0.6	1.4	M140	4.1	12.1
$\beta 5$ - $\alpha 6/\alpha 6$	TS1/22	Q266, S270	3.9	9.4	H264	6.6	7.2
$\beta 5$ - $\alpha 6/\alpha 6$	TS2/14	S270, E272	3.0	6.9	H264	7.8	9.7
$\beta 5$ - $\alpha 6/\alpha 6$	25-3-1	Q266, T267, K286, S270, E272	3.8	9.1	H264	6.6	9.6
$\beta 3$ - $\alpha 2/\alpha 4$	MEM83	D182, E218	0.5	1.0	N207	14.1	17.1

<sup>a</sup> The structures shown in Table IV were superimposed on 1LFA using residues 130–239, 241–260, and 274–277. In case of independent molecules in the asymmetric unit, the first in the protein data bank file or model 15 of 1DGQ were used. The C $\alpha$  atom coordinates were placed in an Excel worksheet. The mean and maximum values were determined from all pairwise comparisons between structures, of the distance between equivalent C $\alpha$  atoms in the superimposed structures, averaged over each epitope residue. Distances rather than root mean square deviations were determined. Distances of the nearest ICAM-1 contact residue to epitope residues were determined using the structure of the  $\alpha_L$  I domain bound to ICAM-1 (6).

for inhibiting binding of ICAM-1. Thus, there is a plausible mechanism for explaining allosteric inhibition by mAb to  $\beta 5$ - $\alpha 6$  epitopes. Second, as stated above and shown in Table V, residues in the  $\beta 5$ - $\alpha 6/\alpha 6$  epitope can be quite near the ICAM-1 contact site; however, because of the flexibility in this region, Abs could bind to and stabilize markedly different conformations of the loop, with some Abs overlapping the contact site, and others not. Third, in contrast to the  $\beta 1$ - $\alpha 1/\alpha 3$ - $\alpha 4$  epitopes, ICAM-1 binds with an orientation such that noncontacting regions of domains 1 and 2 of ICAM-1 are far from the  $\beta 5$ - $\alpha 6/\alpha 6$  epitopes (Fig. 2). Therefore, there is much less scope for regions outside of the Ag binding site of a bound Fab moiety to clash with a bound ICAM-1, and thereby give competitive inhibition. Docking of a Fab using molecular graphics showed that only particular orientations clashed (data not shown).

The agonistic mAb MEM83 (17, 19) recognizes residue Asp<sup>182</sup> on the  $\beta 3$ - $\alpha 2$  loop, and Glu<sup>218</sup> at the end of the  $\alpha 4$  helix. These residues are located on a face of the  $\alpha_L$  I domain opposite from and distant from the ligand binding site, and close to the bottom of the I domain that interfaces with the  $\beta$ -propeller domain (Fig. 2). There is no significant conformational change in the mAb MEM83 epitope, with mean and maximum displacements of 0.5 and 1.0 Å between the eight structures (Table V). Furthermore, the conformation of this region is not correlated with shape-shifting at the ligand binding site. Therefore, agonism by MEM83 appears to be accounted for by its effect on the relative orientation of domains within the  $\alpha_L\beta_2$  heterodimer. Mutations at the bottom of the  $\alpha_M$  and  $\alpha_L$  I domains activate  $\alpha_M\beta_2$  and  $\alpha_L\beta_2$  (40–43), suggesting that the bottom side of the I domain that connects to the  $\beta$ -propeller domain regulates ligand binding by the I domain. It is likely that mAb MEM83 activates LFA-1 binding to ICAM-1 by changing the orientation of the I domain relative to other domains in the  $\alpha_L\beta_2$  heterodimer, which could possibly lead indirectly to conformational change within the I domain at the ICAM-1 binding site.

In summary, our study illustrates diverse mechanisms whereby Abs can activate or inhibit ligand binding by conformationally regulated surface molecules. A rich dataset of eight independent  $\alpha_L$  I domain structures has allowed us to interpret the epitope mapping data presented in this study. The results explain how one group of six mAbs that bind to a conformationally stable region of the  $\alpha_L$  I domain in the  $\beta 1$ - $\alpha 1$  and  $\alpha 3$ - $\alpha 4$  loops, despite some differences in the precise constellation of residues recognized in this region, always strongly inhibit ligand binding. They explain

the effects of another group of three mAbs, which bind almost as close to the ligand binding site but on the opposite side of the MIDAS, to the  $\beta 5$ - $\alpha 6$  loop and  $\alpha 6$  helix. This region is conformationally highly plastic as shown by the influence of crystal lattice contacts, and has some coupling to conformational change at the ligand binding site that regulates affinity for ICAM-1. This explains why these three mAb behave so differently, with one appearing to be a competitive inhibitor, and the other two appearing to be mixed or noncompetitive inhibitors. Finally, the agonistic mAb binds distant to the ligand binding site to a region that does not undergo significant conformational change, suggesting that it alters interdomain relationships within  $\alpha_L\beta_2$  heterodimers. A full explanation for the agonistic effect of MEM83 mAb will require a structure of the full  $\alpha_L\beta_2$  ectodomain, or at least its ligand-binding headpiece.

## Acknowledgments

We thank T. Xiao for figure preparation, and W. Yang for additional experiments.

## References

- Larson, R. S., and T. A. Springer. 1990. Structure and function of leukocyte integrins. *Immunol. Rev.* 114:181.
- Gahmberg, C. G., M. Tolvanen, and P. Kotovuori. 1997. Leukocyte adhesion: structure and function of human leukocyte  $\beta_2$ -integrins and their cellular ligands. *Eur. J. Biochem.* 245:215.
- Carman, C. V., and T. A. Springer. 2003. Integrin avidity regulation: are changes in affinity and conformation underemphasized? *Curr. Opin. Cell Biol.* 15:547.
- Shimaoka, M., J. Takagi, and T. A. Springer. 2002. Conformational regulation of integrin structure and function. *Annu. Rev. Biophys. Biomol. Struct.* 31:485.
- Emsley, J., C. G. Knight, R. W. Farndale, M. J. Barnes, and R. C. Liddington. 2000. Structural basis of collagen recognition by integrin  $\alpha 2\beta 1$ . *Cell* 101:47.
- Shimaoka, M., T. Xiao, J.-H. Liu, Y. Yang, Y. Dong, C.-D. Jun, A. McCormack, R. Zhang, A. Joachimiak, J. Takagi, et al. 2003. Structures of the  $\alpha_L$  I domain and its complex with ICAM-1 reveal a shape-shifting pathway for integrin regulation. *Cell* 112:99.
- Lu, C., M. Shimaoka, M. Ferzly, C. Oxvig, J. Takagi, and T. A. Springer. 2001. An isolated, surface-expressed I domain of the integrin  $\alpha_L\beta_2$  is sufficient for strong adhesive function when locked in the open conformation with a disulfide. *Proc. Natl. Acad. Sci. USA* 98:2387.
- Shimaoka, M., C. Lu, R. Palframan, U. H. von Andrian, J. Takagi, and T. A. Springer. 2001. Reversibly locking a protein fold in an active conformation with a disulfide bond: integrin  $\alpha_L$  I domains with high affinity and antagonist activity in vivo. *Proc. Natl. Acad. Sci. USA* 98:6009.
- Labadia, M. E., D. D. Jeanfavre, G. O. Caviness, and M. M. Morelock. 1998. Molecular regulation of the interaction between leukocyte function-associated antigen-1 and soluble ICAM-1 by divalent metal cations. *J. Immunol.* 161:836.
- Qu, A., and D. J. Leahy. 1995. Crystal structure of the I-domain from the CD11a/CD18 (LFA-1,  $\alpha_L\beta_2$ ) integrin. *Proc. Natl. Acad. Sci. USA* 92:10277.
- Qu, A., and D. J. Leahy. 1996. The role of the divalent cation in the structure of the I domain from the CD11a/CD18 integrin. *Structure* 4:931.

12. Kallen, J., K. Welzenbach, P. Ramage, D. Geyl, R. Kriwacki, G. Legge, S. Cottens, G. Weitz-Schmidt, and U. Hommel. 1999. Structural basis for LFA-1 inhibition upon lovastatin binding to the CD11a I-domain. *J. Mol. Biol.* 292:1.
13. Legge, G. B., R. W. Kriwacki, J. Chung, U. Hommel, P. Ramage, D. A. Case, H. J. Dyson, and P. E. Wright. 2000. NMR solution structure of the inserted domain of human leukocyte function associated antigen-1. *J. Mol. Biol.* 295:1251.
14. Huang, C., and T. A. Springer. 1995. A binding interface on the I domain of lymphocyte function associated antigen-1 (LFA-1) required for specific interaction with intercellular adhesion molecule 1 (ICAM-1). *J. Biol. Chem.* 270:19008.
15. Huang, C., and T. A. Springer. 1995. Domain localization and correlation with inhibition of function of workshop CD11a mAb. In *Leucocyte Typing V: White Cell Differentiation Antigens*. S. F. Schlossman, L. Boumsell, W. Gilks, J. Harlan, T. Kishimoto, T. Morimoto, J. Ritz, S. Shaw, R. Silverstein, T. Springer, T. Tedder, and R. Todd, eds. Oxford Univ. Press, New York, p. 1595.
16. Huang, C., Q. Zang, J. Takagi, and T. A. Springer. 2000. Structural and functional studies with antibodies to the integrin  $\beta 2$  subunit: a model for the I-like domain. *J. Biol. Chem.* 275:21514.
17. Landis, R. C., R. I. Bennett, and N. Hogg. 1993. A novel LFA-1 activation epitope maps to the I domain. *J. Cell Biol.* 120:1519.
18. Lu, C., M. Shimaoka, Q. Zang, J. Takagi, and T. A. Springer. 2001. Locking in alternate conformations of the integrin  $\alpha_L\beta_2$  I domain with disulfide bonds reveals functional relationships among integrin domains. *Proc. Natl. Acad. Sci. USA* 98:2393.
19. Bazil, V., I. Stefanova, I. Hilgert, H. Kristofova, S. Vanek, and V. Horejsi. 1990. Monoclonal antibodies against human leukocyte antigens. IV. Antibodies against subunits of the LFA-1 (CD11a/CD18) leukocyte-adhesion glycoprotein. *Folia Biol. (Praha)* 36:41.
20. Fischer, A., W. Friedrich, A. Fasth, S. Blanche, F. Le Deist, D. Girault, F. Veber, J. Vossen, M. Lopez, C. Griscelli, and M. Hirn. 1991. Reduction of graft failure by a monoclonal antibody (anti-LFA-1 CD11a) after HLA nonidentical bone marrow transplantation in children with immunodeficiencies, osteopetrosis, and Fanconi's anemia: a European group for immunodeficiency/European group for bone marrow transplantation report. *Blood* 77:249.
21. Gordon, K. B., K. A. Papp, T. K. Hamilton, P. A. Walicke, W. Dummer, N. Li, B. W. Bresnahan, and A. Menter. 2003. Efalizumab for patients with moderate to severe plaque psoriasis: a randomized controlled trial. *J. Am. Med. Assoc.* 290:3073.
22. Sanchez-Madrid, F., A. M. Krensky, C. F. Ware, E. Robbins, J. L. Strominger, S. J. Burakoff, and T. A. Springer. 1982. Three distinct antigens associated with human T lymphocyte-mediated cytotoxicity: LFA-1, LFA-2, and LFA-3. *Proc. Natl. Acad. Sci. USA* 79:7489.
23. Ohashi, Y., S. Tsuchiya, H. Fujie, M. Minegishi, and T. Konno. 1992. Anti-LFA-1 antibody treatment of a patient with steroid-resistant severe graft-versus-host disease. *J. Exp. Med.* 167:297.
24. Fischer, A., S. Blanche, F. Veber, M. Delaage, C. Mawas, C. Griscelli, F. Le Deist, M. Lopez, D. Olive, and G. Janossy. 1986. Prevention of graft failure by an anti-HLFA-1 monoclonal antibody in HLA-mismatched bone-marrow transplantation. *Lancet* 2:1058.
25. Petruzzelli, L., J. Luk, and T. A. Springer. 1995. Adhesion structure subpanel 5, leukocyte integrins: CD11a, CD11b, CD11c, CD18. In *Leucocyte Typing V: White Cell Differentiation Antigens*. S. F. Schlossman, L. Boumsell, W. Gilks, J. Harlan, T. Kishimoto, T. Morimoto, J. Ritz, S. Shaw, R. Silverstein, T. Springer, T. Tedder, and R. Todd, eds. Oxford Univ. Press, New York, p. 1581.
26. Springer, T. A., E. Luther, and L. B. Klickstein. 1995. Adhesion structures: section report. In *Leucocyte Typing V: White Cell Differentiation Antigens*. S. F. Schlossman, L. Boumsell, W. Gilks, J. Harlan, T. Kishimoto, T. Morimoto, J. Ritz, S. Shaw, R. Silverstein, T. Springer, T. Tedder, and R. Todd, eds. Oxford University Press, New York, p. 1443.
27. Ho, S. N., H. D. Hunt, R. M. Horton, J. K. Pullen, and L. R. Pease. 1989. Site-directed mutagenesis by overlap extension using the polymerase chain reaction. *Gene* 77:51.
28. Horton, R. M., Z. Cai, S. N. Ho, and L. R. Pease. 1990. Gene splicing by overlap extension: tailor-made genes using the polymerase chain reaction. *BioTechniques* 8:528.
29. Lu, C., M. Ferzly, J. Takagi, and T. A. Springer. 2001. Epitope mapping of antibodies to the C-terminal region of the integrin  $\beta 2$  subunit reveals regions that become exposed upon receptor activation. *J. Immunol.* 166:5629.
30. Huang, C., and T. A. Springer. 1997. Folding of the  $\beta$ -propeller domain of the integrin  $\alpha_L$  subunit is independent of the I domain and dependent on the  $\beta_2$  subunit. *Proc. Natl. Acad. Sci. USA* 94:3162.
31. Champe, M., B. W. McIntyre, and P. W. Berman. 1995. Monoclonal antibodies that block the activity of leukocyte function-associated antigen 1 recognize three discrete epitopes in the inserted domain of CD11a. *J. Biol. Chem.* 270:1388.
32. Hildreth, J. E. K., F. M. Gotch, P. D. K. Hildreth, and A. J. McMichael. 1983. A human lymphocyte-associated antigen involved in cell-mediated lympholysis. *Eur. J. Immunol.* 13:202.
33. Gottlieb, A. B., J. G. Krueger, K. Wittkowski, R. Dedrick, P. A. Walicke, and M. Garovoy. 2002. Psoriasis as a model for T-cell-mediated disease: immunobiologic and clinical effects of treatment with multiple doses of efalizumab, an anti-CD11a antibody. *Arch. Dermatol.* 138:591.
34. Lo Conte, L., C. Chothia, and J. Janin. 1999. The atomic structure of protein-protein recognition sites. *J. Mol. Biol.* 285:2177.
35. Sanchez-Madrid, F., D. Davignon, E. Martz, and T. A. Springer. 1982. Antigens involved in mouse cytolytic T-lymphocyte (CTL)-mediated killing: functional screening and topographic relationship. *Cell. Immunol.* 73:1.
36. Trowbridge, I. S., and M. B. Omary. 1981. Molecular complexity of leukocyte surface glycoproteins related to the macrophage differentiation antigen Mac-1. *J. Exp. Med.* 154:1517.
37. Harning, R., J. Pelletier, K. Lubbe, F. Takei, and V. J. Merluzzi. 1991. Reduction in the severity of graft-versus-host disease and increased survival in allogeneic mice by treatment with monoclonal antibodies to cell adhesion antigens LFA-1 $\alpha$  and MALA-2. *Transplantation* 52:842.
38. Gadek, T. R., D. J. Burdick, R. S. McDowell, M. S. Stanley, J. C. Marsters, Jr., K. J. Paris, D. A. Oare, M. E. Reynolds, C. Ladner, K. A. Zioncheck, et al. 2002. Generation of an LFA-1 antagonist by the transfer of the ICAM-1 immunoregulatory epitope to a small molecule. *Science* 295:1086.
39. Yang, W., M. Shimaoka, J. F. Chen, and T. A. Springer. 2004. Activation of integrin  $\beta$  subunit I-like domains by one-turn C-terminal  $\alpha$ -helix deletions. *Proc. Natl. Acad. Sci. USA* 101:2333.
40. Oxvig, C., C. Lu, and T. A. Springer. 1999. Conformational changes in tertiary structure near the ligand binding site of an integrin I domain. *Proc. Natl. Acad. Sci. USA* 96:2215.
41. Huth, J. R., E. T. Olejniczak, R. Mendoza, H. Liang, E. A. Harris, M. L. Lupher, Jr., A. E. Wilson, S. W. Fesik, and D. E. Staunton. 2000. NMR and mutagenesis evidence for an I domain allosteric site that regulates lymphocyte function-associated antigen 1 ligand binding. *Proc. Natl. Acad. Sci. USA* 97:5231.
42. Zhang, L., and E. F. Plow. 1999. Amino acid sequences within the  $\alpha$  subunit of integrin  $\alpha_M\beta_2$  (Mac-1) critical for specific recognition of C3bi. *Biochemistry* 38:8064.
43. Alonso, J. L., M. Essafi, J. P. Xiong, T. Stehle, and M. A. Arnaout. 2002. Does the integrin  $\alpha_A$  domain act as a ligand for its  $\beta_A$  domain? *Curr. Biol.* 12:R340.
44. Nicholls, A., K. A. Sharp, and B. Honig. 1991. Protein folding and association: insights from the interfacial and thermodynamic properties of hydrocarbons. *Proteins* 11:281.
45. Esnouf, R. M. 1997. An extensively modified version of MolScript that includes greatly enhanced coloring capabilities. *J. Mol. Graph. Model.* 15:132.
46. Merritt, E. A., and M. E. P. Murphy. 1994. Raster 3D version 2.0: a program for photorealistic graphics. *Acta Crystallogr. D* 50:869.